

$\alpha 7$ -nAChR Knockout Mice Decreases Biliary Hyperplasia and Liver Fibrosis in Cholestatic Bile Duct-Ligated Mice

Laurent Ehrlich,* April O'Brien,† Chad Hall,‡ Tori White,† Lixian Chen,* Nan Wu,* Julie Venter,* Marinda Scrushy,* Muhammad Mubarak,* Fanyin Meng,*†§ David Dostal,* Chaodong Wu,¶ Terry C. Lairmore,‡ Gianfranco Alpini,*†§ and Shannon Glaser*†§

*Department of Medical Physiology, Baylor Scott & White and Texas A&M University Health Science Center, Temple, TX, USA

†Research, Central Texas Veterans Health Care System, Temple, TX, USA

‡Surgery, Baylor Scott & White and Texas A&M University Health Science Center, Temple, TX, USA

§Gastroenterology, Baylor Scott & White Digestive Disease Research Center, Baylor Scott & White, Temple, TX, USA

¶Department of Nutrition and Food Science, Texas A&M University, College Station, TX, USA

$\alpha 7$ -nAChR is a nicotinic acetylcholine receptor [specifically expressed on hepatic stellate cells (HSCs), Kupffer cells, and cholangiocytes] that regulates inflammation and apoptosis in the liver. Thus, targeting $\alpha 7$ -nAChR may be therapeutic in biliary diseases. Bile duct ligation (BDL) was performed on wild-type (WT) and $\alpha 7$ -nAChR^{-/-} mice. We first evaluated the expression of $\alpha 7$ -nAChR by immunohistochemistry (IHC) in liver sections. IHC was also performed to assess intrahepatic bile duct mass (IBDM), and Sirius Red staining was performed to quantify the amount of collagen deposition. Immunofluorescence was performed to assess colocalization of $\alpha 7$ -nAChR with bile ducts (costained with CK-19) and HSCs (costained with desmin). The mRNA expression of $\alpha 7$ -nAChR, Ki-67/PCNA (proliferation), fibrosis genes (TGF- $\beta 1$, fibronectin-1, Col1 $\alpha 1$, and α -SMA), and inflammatory markers (IL-6, IL-1 β , and TNF- α) was measured by real-time PCR. Biliary TGF- $\beta 1$ and hepatic CD68 (Kupffer cell marker) expression was assessed using IHC. $\alpha 7$ -nAChR immunoreactivity was observed in both bile ducts and HSCs and increased following BDL. $\alpha 7$ -nAChR^{-/-} BDL mice exhibited decreased (i) bile duct mass, liver fibrosis, and inflammation, and (ii) immunoreactivity of TGF- $\beta 1$ as well as expression of fibrosis genes compared to WT BDL mice. $\alpha 7$ -nAChR activation triggers biliary proliferation and liver fibrosis and may be a therapeutic target in managing extrahepatic biliary obstruction.

Key words: Nicotine; Biliary epithelium; Fibrosis; Cholinergic; Cholestasis

INTRODUCTION

Cholangiocytes are epithelial cells that line the bile duct system and are the main targets of cholangiopathies^{1,2}. Cholangiopathies, while broad in etiology, are characterized by cholestasis, ductular reaction, and liver fibrosis^{2,3}. Extrahepatic bile duct obstruction, mimicked by bile duct ligation (BDL), increases pressure across the biliary tree leading to increased intrahepatic bile duct mass (IBDM) and bridging fibrosis between intrahepatic portal triads^{4,5}. In contrast, primary sclerosing cholangitis (PSC), a well-known autoimmune cholangiopathy, results in irregular bile duct proliferation, periductal fibrosis, and bridging necrosis, which progresses to cirrhosis and the need for liver transplantation⁶⁻⁹.

Vagal stimulation of the hepatic cholinergic system is anti-inflammatory and antiapoptotic and is strongly

mediated by $\alpha 7$ nicotinic acetylcholine receptor ($\alpha 7$ -nAChR) activation^{10,11}. It is important to recognize distinct dynamics between nicotine and acetylcholine, the endogenous physiological stimulants of nAChRs. While extracellular acetylcholine is quickly degraded by acetylcholinesterases (small fraction of a second), nicotine has a much longer half-life (~2 h) and therefore stimulates nAChR for a longer time period before being degraded and cleared¹². Acetylcholine also acts through muscarinic acetylcholine receptors (mAChRs), while nicotine does not, to drive cholangiocyte proliferation and secretin-dependent choleresis in a cAMP-dependent fashion following BDL¹³ and hepatic stellate cell (HSC) activation and fibrogenesis in a PI3K- and MEK-dependent pathway¹⁴.

There remains considerable controversy on the effects of smoking and the pathogenesis of certain biliary diseases,

Address correspondence to Shannon Glaser, Ph.D., Associate Professor, Medical Physiology, Baylor Scott & White Digestive Disease Research Center, Central Texas Veterans University Health Care System, Texas A & M Health Science Center, Olin E. Teague Medical Center, 1901 South 1st Street, Building 205, Temple, TX 76504, USA. Tel: 254-743-1044; Fax: 254-743-0378; E-mail: sglaser@medicine.tamhsc.edu

particularly PSC¹⁵. In particular, there is small but significant epidemiological data indicating that smoking may be protective in PSC patients who are male or who have concomitant ulcerative colitis (UC)^{15,16}. Patients with PSC are less likely to smoke, and male daily smokers experienced later onset of disease compared to nonsmoking male counterparts¹⁵. While smoking may increase the incidence of cholangiocarcinoma (CCA) in patients with PSC, it may be protective in the subtype of PSC with concomitant inflammatory bowel disease (IBD)^{17,18}. Of course, smoking increases the incidence of colorectal cancer in patients with IBD, which is in itself a risk factor for CCA onset.

With regard to extrahepatic causes of cholestasis, smoking is not associated with onset of gallstones; however, smoking is an independent risk factor for the onset of gallbladder cancer in patients with underlying gallstones¹⁹. We have previously shown that rats treated with nicotine by osmotic minipumps exhibited increased cholangiocyte proliferation, which is consistent with its procholinergeric, anti-inflammatory, and antiapoptotic effects²⁰. Nicotine treatment also increased expression of fibrotic genes and $\alpha 7$ -nicotinic receptor²⁰. We have also shown that nicotine increases growth and proliferation of CCA xenograft tumors, which is abrogated in $\alpha 7$ -nAChR^{-/-} CCA tumors²¹. In this article, we sought to characterize the role of $\alpha 7$ -nAChR in BDL mice, a model of extrahepatic cholestasis characterized by increased biliary proliferation and liver fibrosis.

MATERIALS AND METHODS

Materials

Reagents were purchased from Sigma-Aldrich (St. Louis, MO, USA) unless otherwise indicated. The following antibodies were purchased from Abcam (Cambridge, MA, USA): $\alpha 7$ -nAChR (ab24644), desmin (Y66; Alexa Fluor 488), cytokeratin-19 (CK-19; ab52625), and transforming growth factor- $\beta 1$ (TGF- $\beta 1$; ab92486). All the following mouse primers were purchased from Qiagen (Valencia, CA, USA): $\alpha 7$ -nAChR (Chrna7; NM_007390), CK-19 (NM_008471), Ki-67 (NM_001081117), collagen type I $\alpha 1$ (Col1 $\alpha 1$; NM_007742), fibronectin-1 (Fn-1; NM_010233), α -smooth muscle actin (α -SMA; NM_007392), TGF- $\beta 1$ (NM_011577), interleukin-6 (IL-6; NM_031168), IL-1 β (NM_008361), tumor necrosis factor- α (TNF- α , NM_013693), CYP7A1 (NM_178847), cholesterol 7 α -hydroxylase (CYP27A1; NM_178847), bile salt export pump (BSEP; NM_031760), and the housekeeping glyceraldehyde-3-phosphate dehydrogenase (GAPDH; NM_008084). PerCP and Alexa Fluor 488 secondary antibodies used in immunofluorescence were purchased from Jackson ImmunoResearch (West Grove, PA, USA). TGF- $\beta 1$ ELISA kits were purchased from Invitrogen (88-8350-22; Carlsbad, CA, USA).

In Vivo Studies

Animal Models. Animal protocols were approved by the Baylor Scott & White Institutional Animal Care and Use Committee. Male C57BL/6 [wild type (WT), 12 weeks of age, 25–30 g] and $\alpha 7$ -nAChR^{-/-} mice (12 weeks of age, 25–30 g) were purchased from Jackson Laboratory (Bar Harbor, ME, USA), housed in a temperature-controlled environment (22°C) with 12-h:12-h light–dark cycles, and fed standard rodent chow with free access at water ad libitum. Briefly, the last exons of the *Chrna7* gene were deleted and a knockout (KO) mouse was generated on a mixed 129/SvEv and C57BL/6 background and eventually bred to a C57BL/6 background. Our studies were performed in four groups of animals: (i) normal WT and $\alpha 7$ -nAChR^{-/-} mice, and (ii) WT and $\alpha 7$ -nAChR^{-/-} mice that underwent BDL surgery²² for 7 days. From these groups of animals, total liver samples were harvested and used for the preparation of frozen or paraffin-embedded liver sections.

Immunoreactivity for $\alpha 7$ -nAChR, TGF- $\beta 1$, and Cluster of Differentiation 68 (CD68), and Measurement of Biliary Proliferation, Intrahepatic Bile Duct Mass (IBDM), and Liver Fibrosis. Immunohistochemistry (IHC) for $\alpha 7$ -nAChR, TGF- $\beta 1$, and CD68 was performed on paraffin-embedded liver sections (4–5 μ m) from the selected groups of mice as previously described²³. Biliary TGF- $\beta 1$ immunoreactivity was measured in intrahepatic bile ducts as the staining intensity per bile duct field using the Olympus Image Pro-Analyzer software (Olympus, Tokyo, Japan); values were normalized to normal WT liver sections. Anti-CD68 antibody (ab125212) was used for liver Kupffer cell identification by IHC on paraffin-embedded liver sections from the selected groups of mice²⁴. We also evaluated by immunofluorescence in frozen liver sections (4–5 μ m thick) the expression of $\alpha 7$ -nAChR in bile ducts (costained with CK-19, a cholangiocyte-specific marker)²² as well as HSCs (costained with desmin, a marker of HSCs)²⁵. Following staining, slides were mounted with DAPI (Invitrogen), to stain for cell nuclei, and imaged with a confocal microscope (FluoView 500 laser scan microscope with DP70 digital camera; Olympus). CK-19 values were normalized to normal WT sections; $\alpha 7$ -nAChR basal expression in normal WT slides was too low to normalize; therefore, values were expressed as relative changes.

IBDM was measured in paraffin-embedded liver sections (4–5 μ m thick, 10 fields analyzed from three samples from three different animals) as the area occupied by the CK-19⁺ bile ducts/total area $\times 100$. Sections were examined by the Olympus Image Pro-Analyzer software (Olympus).

We measured liver fibrosis by (i) Sirius Red staining in liver sections (4–5 μ m thick, 10 fields analyzed from

three different samples from three different animals), and (ii) measurement of hydroxyproline levels in total liver samples using the Hydroxyproline Assay Kit (MAK008; Sigma-Aldrich). Following Sirius Red staining, slides were scanned by a digital scanner (SCN400; Leica Microsystems, Buffalo Grove, IL, USA) and quantified using Image-Pro Premier 9.1 (Media Cybernetics, MD, USA).

Real-Time PCR. Mouse cholangiocytes were obtained by immunoaffinity separation as previously described^{13,22}. The immortalized, nonmalignant, cholangiocyte cell line H69 (where we perform the *in vitro* stretch experiments) was obtained from Dr. G. J. Gores of Mayo Clinic (Rochester, MN, USA)²⁶. Total RNA was isolated from snap-frozen samples from total liver, cholangiocytes, or H69 cells using the Ambion *mirVana*TM Isolation Kit (Ambion, Austin, TX, USA) as previously described²³. cDNA was created with 5x *iScript*TM Supermix (Bio-Rad, Hercules, CA, USA) according to the vendor's protocol. Real-time PCR analysis of the selected samples was performed using 1 μ g of total RNA with the SYBR Green Real-Time PCR Kit (SABiosciences, Frederick, MD, USA) with GAPDH as housekeeping gene²³.

In Vitro Stretch Experiment in Human Cholangiocyte Lines

H69 cells were plated on Flexcell[®] six-well membrane plates (Flexcell[®], Burlington, NC, USA) at 200,000 cells/700 μ l of media, serum starved for 24 h, and subjected to biaxial mechanical stress on the Flexcell[®] FXSKTM Tension System for 24 h (Flexcell[®])²⁷. Controls were plated on the same plates but not subjected to mechanical stress. Supernatant was collected, and protein levels of TGF- β 1 were evaluated using an ELISA kit (Invitrogen).

RESULTS

Expression of α 7-nAChR

There was increased immunoreactivity for α 7-nAChR in liver sections from BDL WT compared to WT mice; immunoreactivity for α 7-nAChR was absent in both normal and BDL α 7-nAChR^{-/-} mice (Fig. 1A and B). The localization of α 7-nAChR in intrahepatic bile ducts (red color costained in green with CK-19) and in HSCs (green color in HSCs costained in red with desmin) was also confirmed by immunofluorescence (Fig. 1C–E).

α 7-nAChR^{-/-} Mice Exhibit Lower Biliary Proliferation and IBDM Following BDL

There was increased IBDM in BDL WT compared to normal WT mice. However, there was a significant decrease in IBDM in α 7-nAChR^{-/-} BDL compared to WT BDL (Fig. 2A). BDL-induced increase in Ki-67A mRNA expression was reduced in total liver samples

from α 7-nAChR^{-/-} BDL compared to WT BDL mice (Fig. 2); no significant differences in these parameters were observed between normal WT and α 7-nAChR^{-/-} mice (Fig. 2B).

Liver Fibrosis Is Decreased in α 7-nAChR^{-/-} Mice Following BDL

Sirius Red staining for collagen deposition and hydroxyproline levels both increased in WT BDL compared to normal WT mice but decreased in α 7-nAChR^{-/-} BDL mice compared to WT BDL (Fig. 3A and B). Additionally, gene expression of the fibrosis markers α -SMA, TGF- β 1, Col1 α 1, and Fn-1 decreased in total liver samples from α 7-nAChR^{-/-} BDL mice compared to WT BDL mice (Fig. 4). No significant differences in collagen content and fibrosis mRNA expression were observed between normal WT and α 7-nAChR^{-/-} mice (Figs. 3 and 4). As shown in Figure 5A, the biliary immunoreactivity of TGF- β 1 greatly increased in liver sections from BDL WT mice (compared to normal WT mice) but was attenuated in α 7-nAChR^{-/-} BDL mice; no significant difference in TGF- β 1 immunoreactivity was observed between normal WT and α 7-nAChR^{-/-} mice. As proof of concept, we subjected H69 cell lines to mechanical stress and measured TGF- β 1 supernatant levels with an ELISA kit. Cholangiocytes indeed secreted more TGF- β 1 (an important signaling factor playing a key role in biliary damage and liver fibrosis)²⁸ following increased mechanical pressure (Fig. 5B).

Kupffer Cell Infiltration and Expression of Inflammatory Markers Are Reduced in α 7-nAChR^{-/-} Mice Following BDL

CD68 immunoreactivity was used to assess Kupffer cell infiltrate from the selected groups of mice. Kupffer cell infiltration increased following BDL but decreased in BDL α 7-nAChR^{-/-} mice (Fig. 6). By real-time PCR, the expression of IL-6, IL-1 β , and TNF- α increased in cholangiocytes from BDL mice (compared to WT mice) but decreased in BDL α 7-nAChR^{-/-} mice compared to BDL WT mice (Fig. 7).

Expression of Bile Acid Synthesis and Transport Genes Reduced in α 7-nAChR^{-/-} Mice Following BDL

The mRNA expression of CYP7A1, CYP27A1, and BSEP (proteins playing important roles in bile acid metabolism)²⁹ increased following BDL and decreased in BDL α 7-nAChR^{-/-} mice (Fig. 8).

DISCUSSION

We have previously shown that chronic nicotine exposure stimulates biliary growth and hepatic fibrosis^{20,21}. In this study, we used total body knockouts of α 7-nAChR to explore its specific effects on a BDL mouse model of

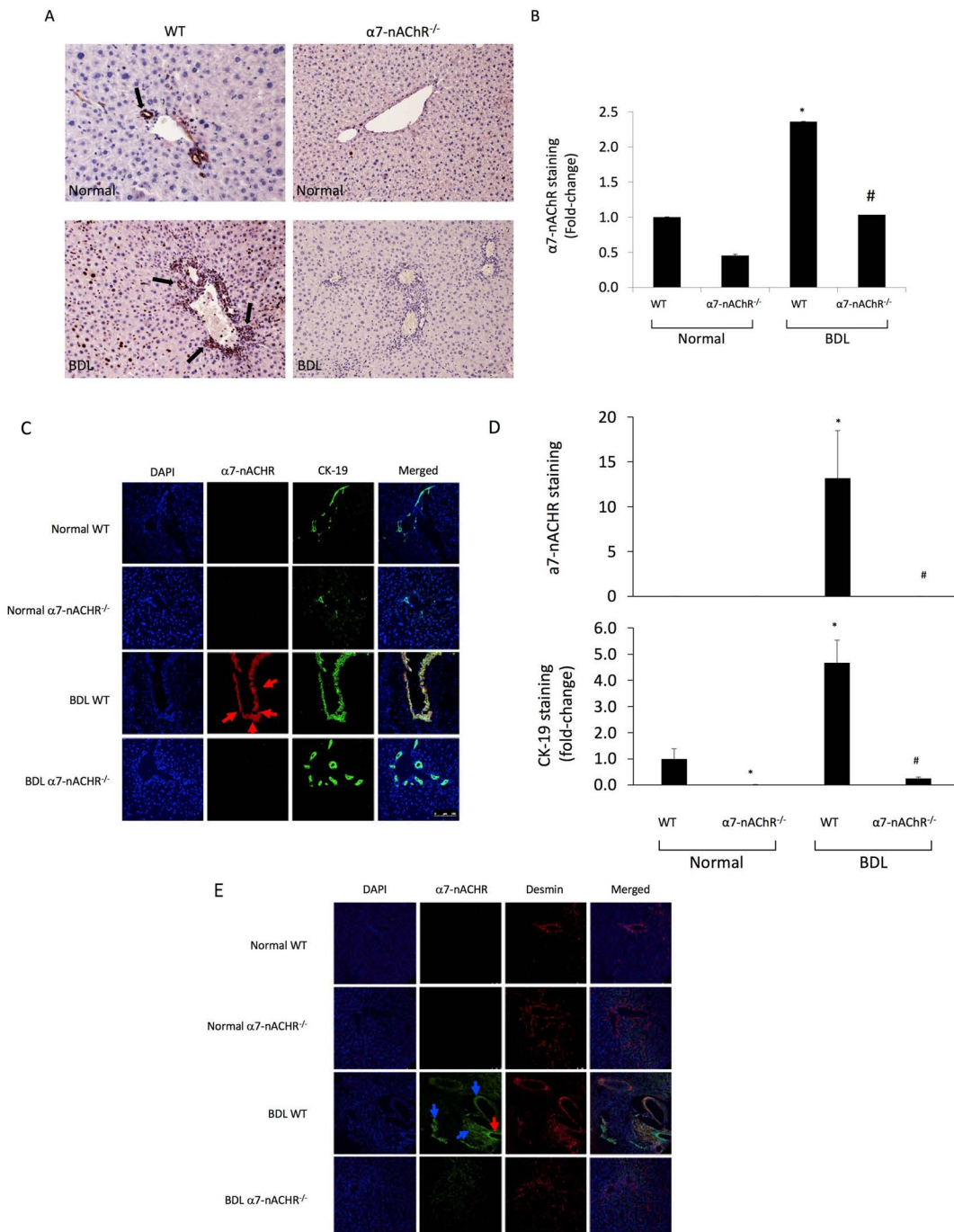


Figure 1. (A, B) Evaluation of the immunoreactivity of $\alpha 7$ nicotinic acetylcholine receptors ($\alpha 7$ -nAChR) in liver sections. There was increased immunoreactivity for $\alpha 7$ -nAChR in liver sections from bile duct ligation (BDL) wild type (WT) compared to WT mice; immunoreactivity for $\alpha 7$ -nAChR was virtually absent in both normal and BDL $\alpha 7$ -nAChR^{-/-} mice. Original magnification: 25 \times . (C–E) By immunofluorescence, we demonstrated the immunoreactivity of $\alpha 7$ -nAChR in bile ducts [red color costained in green with cytokeratin-19 (CK-19)] and in hepatic stellate cells (HSCs; green color in HSCs costained in red with desmin) was also confirmed by immunofluorescence. Blue arrows point to costaining of $\alpha 7$ -nAChR with HSC, while the red arrow most likely represents $\alpha 7$ -nAChR costaining with bile ducts. Nuclei are stained in blue with DAPI. Scale bar: 100 μ m. * p <0.05 versus normal WT mice. # p <0.05 versus BDL WT mice.

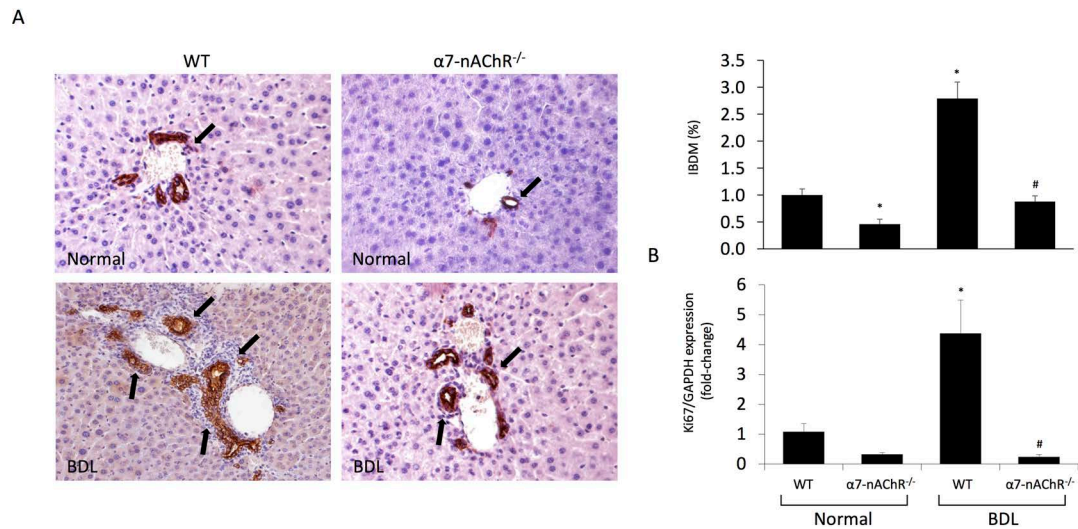


Figure 2. Biliary proliferation and bile duct mass is decreased in $\alpha 7$ -nAChR^{-/-} BDL compared to BDL WT mice. (A) BDL-induced increase in intrahepatic bile duct mass (IBDM) was reduced in BDL $\alpha 7$ -nAChR^{-/-} compared to WT BDL mice. Original magnification: 25 \times . (B) BDL-induced increase in Ki-67A mRNA expression was reduced in total liver samples from $\alpha 7$ -nAChR^{-/-} BDL compared to WT BDL mice. Data are means \pm SEM performed in triplicate in three different total liver samples from three mice. * $p < 0.05$ versus normal WT mice. # $p < 0.05$ versus BDL WT mice.

cholestatic injury. Mice lacking the $\alpha 7$ -nAChR who underwent BDL exhibited reduced bile duct mass and hepatic fibrosis (mediated by receptor-mediated interaction with both cholangiocytes and HSCs) compared to their WT counterparts. We also observed increased immunoreactivity of biliary TGF- $\beta 1$ in liver sections from BDL WT mice

compared to normal WT mice, but reduced immunoreactivity in $\alpha 7$ -nAChR BDL compared to BDL WT mice. Furthermore, we confirmed that $\alpha 7$ -nAChR colocalized with both bile ducts (CK-19) and HSCs (desmin) and that $\alpha 7$ -nAChR^{-/-} BDL mice expressed less activated HSCs compared to WT counterparts. Loss of $\alpha 7$ -nAChR led to

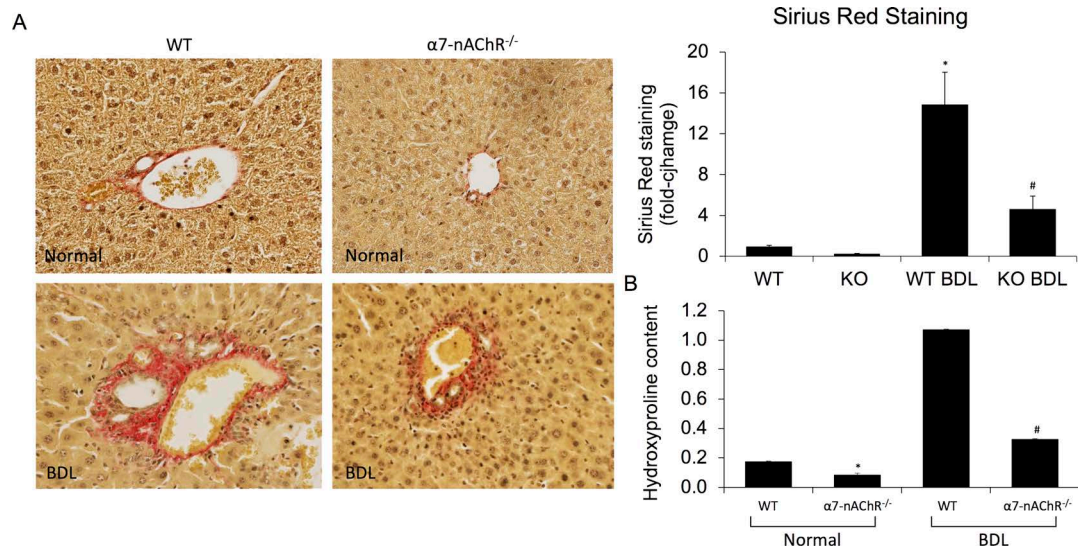


Figure 3. Liver fibrosis is decreased in $\alpha 7$ -nAChR^{-/-} BDL compared to BDL WT mice. By Sirius Red staining for collagen deposition and assay for hydroxyproline levels, liver fibrosis increased in WT BDL compared to normal WT mice but decreased in $\alpha 7$ -nAChR^{-/-} BDL compared to WT BDL mice. (A) Data are means \pm SEM; 10 different fields analyzed from each sample from three different animals. Original magnification: 40 \times . (B) Data are means \pm SEM performed in triplicate in three different total liver samples from three mice. * $p < 0.05$ versus normal WT mice. # $p < 0.05$ versus BDL WT mice.

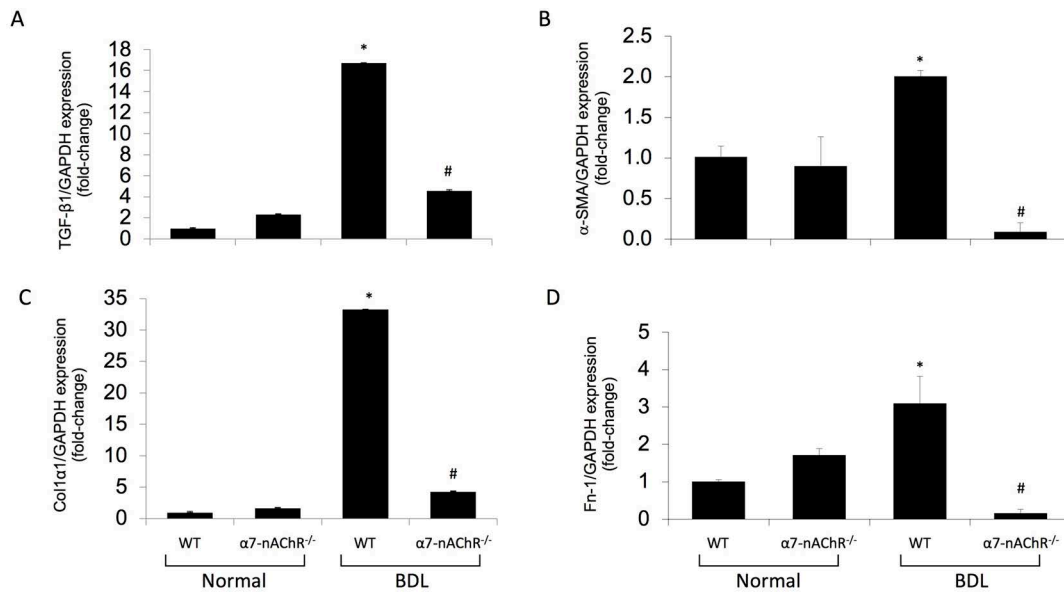


Figure 4. Fibrotic mRNA expression is decreased in $\alpha 7$ -nAChR^{-/-} BDL compared to BDL WT mice. (A–D) Gene expression for α -smooth muscle actin (α -SMA), transforming growth factor- β 1 (TGF- β 1), collagen type I α 1 (Col1 α 1), and fibronectin-1 (Fn-1) increased in total liver samples from WT BDL compared to normal WT mice, but decreased in $\alpha 7$ -nAChR^{-/-} BDL compared to WT BDL mice. Data are means \pm SEM performed in triplicate in three different total liver samples from three mice. * p < 0.05 versus normal WT mice. # p < 0.05 versus BDL WT mice.

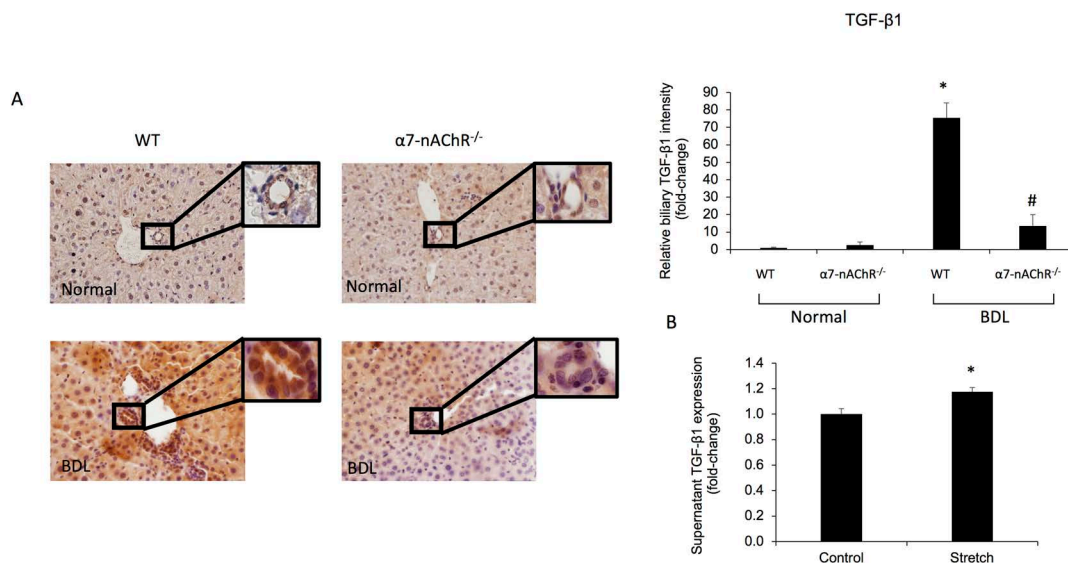


Figure 5. Biliary TGF- β 1 immunoreactivity is decreased in $\alpha 7$ -nAChR^{-/-} BDL compared to BDL WT mice. (A) The immunoreactivity of TGF- β 1 greatly increased in liver sections from BDL WT mice (compared to normal WT mice) but was attenuated in $\alpha 7$ -nAChR^{-/-} BDL mice; no significant difference in TGF- β 1 immunoreactivity was observed between normal WT and $\alpha 7$ -nAChR^{-/-} mice. Original magnification: 40 \times . Scale bar: 100 μ m. (B) Levels of TGF- β 1 were measured in the supernatant of H69 cells subject to biaxial mechanical stress (or control) in order to mimic biliary pressure experienced during BDL in vivo. Biliary TGF- β 1 secretion increased in H69 cells subject to mechanical stretch compared to controls. Data are means \pm SEM performed in triplicate. * p < 0.05 versus control H69.

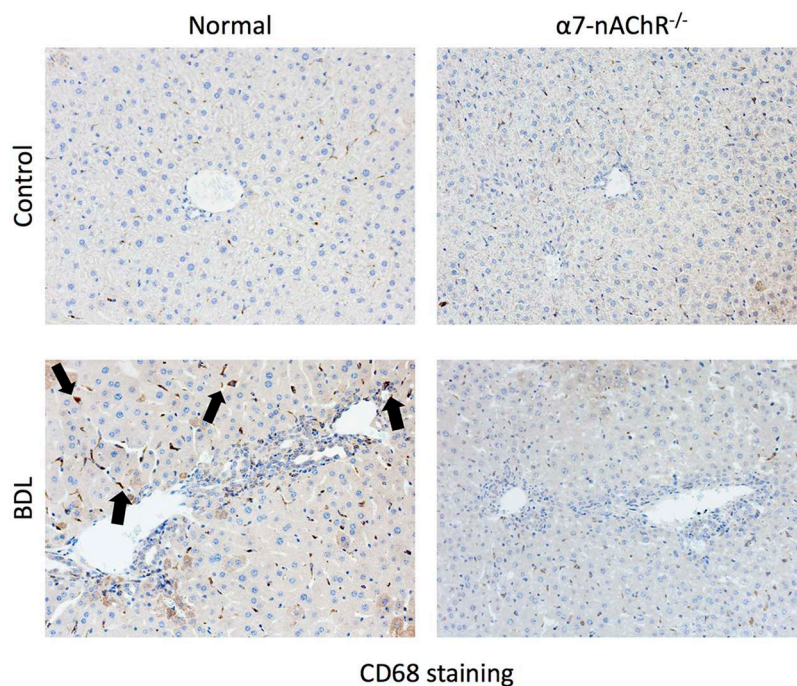


Figure 6. Cluster of differentiation 68 (CD68) immunoreactivity is decreased in $\alpha 7$ -nAChR^{-/-} BDL compared to BDL WT mice. CD68 immunoreactivity was used to assess Kupffer cell infiltration in selected mice groups. The figure shows that Kupffer cell infiltration increases following BDL but decreases in $\alpha 7$ -nAChR^{-/-} BDL mice. Black arrows are used to point out the CD68⁺ Kupffer cells. Original magnification: 20 \times .

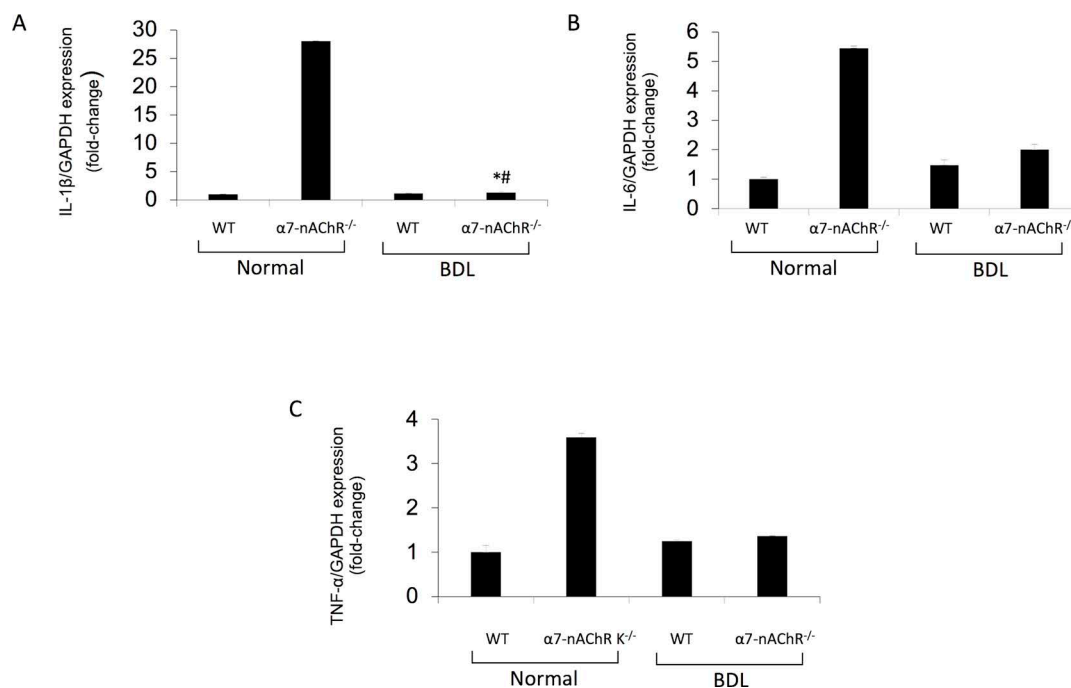


Figure 7. Inflammatory mRNA expression is decreased in $\alpha 7$ -nAChR^{-/-} BDL compared to BDL WT mice. (A–C) Gene expression for interleukin-1 β (IL-1 β), IL-6, and tumor necrosis factor- α (TNF- α) increased in cholangiocytes from WT BDL compared to normal WT mice, but decreased in $\alpha 7$ -nAChR^{-/-} BDL compared to WT BDL mice. Data are means \pm SEM performed in triplicate in three different total liver samples from three mice. * $p < 0.05$ versus normal WT mice. # $p < 0.05$ versus BDL WT mice.

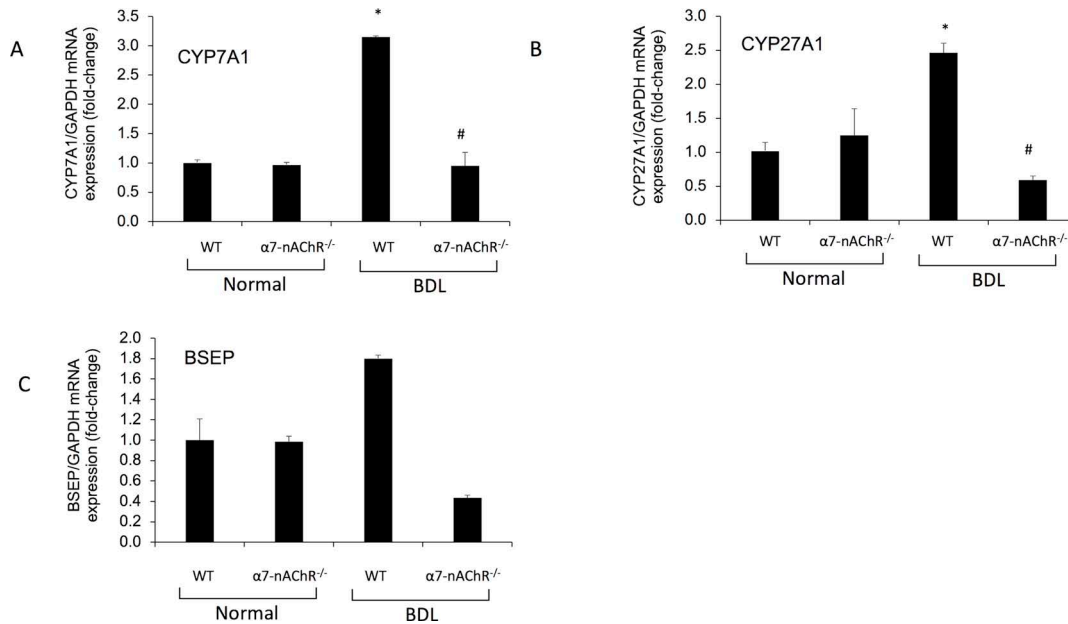


Figure 8. Expression of bile acid synthesis and transport genes reduced in $\alpha 7$ -nAChR^{-/-} mice following BDL. (A–C) Gene expression of CYP7A1, CYP27A1, and bile salt export pump (BSEP) increased following BDL and decreased in BDL $\alpha 7$ -nAChR^{-/-} mice. Data are means \pm SEM performed in triplicate in three different total liver samples from three mice. * $p < 0.05$ versus normal WT mice. # $p < 0.05$ versus BDL WT mice.

decreased Kupffer cell infiltration and reduced expression of bile acid synthesis and transport genes. Thus, in the setting of BDL, $\alpha 7$ -nAChR activation increases Kupffer cell recruitment and even biliary inflammation. On the basis of these findings, we propose that the decrease in biliary proliferation/ductal mass and liver fibrosis is mediated by decreased expression of $\alpha 7$ -nAChR in cholangiocytes and HSCs, respectively. Since we have previously shown that the activation of HSCs and increased liver fibrosis are mediated by enhanced biliary TGF- $\beta 1$ expression/secretion²⁸, we also proposed a paracrine mechanism by which a decrease in biliary TGF- $\beta 1$ immunoreactivity/expression (mediated by KO of $\alpha 7$ -nAChR) contributes to reduced liver fibrosis, potentially through reduced activation of stromal inflammatory cell types such as HSCs and Kupffer cells.

Cigarette smoke is strongly associated with colon and pancreatic cancers, yet epidemiological evidence for its role in liver diseases is less clear, particularly due to confounding factors such as alcohol intake³⁰. While it is generally agreed that smoking contributes to liver disease, particularly hepatocellular carcinoma and CCA, smoking is believed to exacerbate liver injury in partnership with other genetic and environmental insults. For example, smoking is strongly associated with tumorigenesis in patients with chronic hepatitis C, PSC, primary biliary cholangitis (PBC), and gallstones^{19,30}. Cigarette smoke contains over 4,000 chemicals, among which nicotine provides the psychoactive and addictive properties.

There is a host of literature implicating $\alpha 7$ -nAChR as the main player in mediating liver-tropic effects of nicotine^{10,11,20,31,32}. nAChRs are ionotropic, as opposed to G protein-coupled mAChRs, which are metabotropic, and are formed from homo- or heteropentameric assembly of nAChR subunits $\alpha 1$ – 10 , $\beta 1$ – 4 , γ , δ , and ϵ ³³. All forms are present in the central nervous system; however, liver expression of $\alpha 7$ -nAChR is limited to HSCs³², Kupffer cells¹¹, and cholangiocytes²⁰.

$\alpha 7$ -nAChR is part of the vagal cholinergic system that responds to acetylcholine released by postganglionic efferent nerves³⁴, although both nicotinic and muscarinic receptors can bind to acetylcholine. $\alpha 7$ -nAChR expression has been measured in HSCs³², Kupffer cells¹¹, as well as cholangiocytes²⁰. Various mouse models of liver damage have been used to study the effects of vagal stimulation and/or $\alpha 7$ -nAChR activation to somewhat differing conclusions. For example, it is well established that vagal nerve firing releases acetylcholine that binds to $\alpha 7$ -nAChR on Kupffer cells and suppresses IL-6/STAT3 signaling and subsequent hepatic inflammation^{11,35}. Vagal activity further reduces Kupffer cell activation and hepatic inflammation and steatosis in NASH models in an $\alpha 7$ -nAChR-dependent manner³⁶. However, another group showed that nicotine acts directly on the HSC $\alpha 7$ -nAChR axis as well to drive fibrogenesis in NASH models³², and acetylcholine can also bind to muscarinic receptors directly on HSCs and promote a profibrogenic phenotype¹⁴. We have previously shown that nicotine acts

on cholangiocytes in a $\alpha 7$ -nAChR-specific manner to increase biliary proliferation and fibrosis in a Ca⁽²⁺⁾/IP₃/ERK1/2-dependent manner^{20,21}. Thus, it is important to distinguish between nicotine and acetylcholine, nicotinic and muscarinic receptors, and the disease model when trying to determine how biliary proliferation and hepatic fibrosis are affected.

Activated cholangiocytes take on a neuroendocrine-like phenotype that secretes and responds to neuropeptides and hormones in an autocrine and paracrine fashion⁹. In the BDL mouse model, extrahepatic bile duct blockage increases pressure along the biliary tree and causes a toxic buildup of bile acids that leads to biliary damage, ductular reaction, and hepatic fibrosis³⁷. The cholinergic system plays a conflicting role in bile acid homeostasis. In BDL mice models, treatment with the bile acid taurocholate preserved biliary proliferation in rats that underwent hepatic vagotomy through maintenance of apical bile acid transporters in a PI3K/Akt prosurvival-dependent manner³⁸. Cholinergic activation of biliary muscarinic receptors has minimal and variable impact on bile acid secretion and bile acid flow^{39,40}; however, muscarinic receptor activation increases secretin-dependent choleresis through increased Ca⁽²⁺⁾/adenylyl cyclase/Cl⁻/HCO₃⁻ activity⁴¹. In this article, we report that $\alpha 7$ -nAChR^{-/-} BDL expressed lower levels of genes involved in bile acid synthesis and transport²⁹.

Recently, the role of mechanical-induced stress and TGF- β activation, and subsequent fibrosis, has been clarified through its relationship with the $\alpha_v\beta_6$ integrin. Integrin–fibronectin complexes can be activated by increased mechanical stress. Increased binding affinity of the $\alpha_v\beta_6$ integrin associates with latency-associated peptide, which releases latent TGF- β and triggers SMAD phosphorylation and nuclear translocation. Wang et al. demonstrated that $\alpha_v\beta_6$ integrin expression is highly upregulated in cholangiocytes following acute biliary obstruction and that lack of $\alpha_v\beta_6$ integrin expression ameliorated fibrotic phenotype. Additionally, $\alpha_v\beta_6$ integrin is implicated in potential cholangiocyte EMT, presumably toward profibrotic fibroblasts^{42,43}. It is thought that HSCs, or even portal fibroblasts, contribute to the fibrotic reaction through cross-talk with damaged cholangiocytes⁴⁴. HSCs themselves can respond to mechanical pressure by activating and transforming into myofibroblasts during the wound healing process⁴⁴.

We have shown in vivo in BDL mice that loss of $\alpha 7$ -nAChR reduces biliary mass, liver damage, and fibrosis in response to biliary pressure likely due to loss of $\alpha 7$ -nAChR. Furthermore, HSC activation and proliferation are muted following loss of $\alpha 7$ -nAChR. It is possible that loss of $\alpha 7$ -nAChR reduces biliary Ca⁽²⁺⁾ activation, thus blunting the proliferative response. Previous reports demonstrate that $\alpha 7$ -nAChR is profibrotic in HSCs; thus,

loss of $\alpha 7$ -nAChR would reduce HSC activation. We demonstrated that the $\alpha 7$ -nAChR axis increases Kupffer cell infiltrate in the cholestatic BDL mouse model; however, further work is needed to understand how $\alpha 7$ -nAChR affects Kupffer cells in other disease models. Targeting the $\alpha 7$ -nAChR axis may prove therapeutic in the treatment of cholestatic liver diseases and CCA.

ACKNOWLEDGMENTS: *This work was supported by the Dr. Nicholas C. Hightower Centennial Chair of Gastroenterology, Baylor Scott & White, a VA Senior Research Career Scientist Award, a VA Merit award to Dr. Alpini (5101BX000574), a VA Merit Award (5101BX002192) to Dr. Glaser, and a VA Merit Award (1101BX001724) to Dr. Meng from the US Department of Veterans Affairs Biomedical Laboratory Research and Development Service, the NIH grant DK110035 to Dr. Glaser, and the NIH grants DK58411 and DK062975 to Drs. Alpini, Glaser, and Meng. This material is the result of work supported by resources at the Central Texas Veterans Health Care System. The content is the responsibility of the author(s) alone and does not necessarily reflect the views or policies of the Department of Veterans Affairs or the US government. The authors declare no conflicts of interest.*

REFERENCES

1. Lazaridis KN, LaRusso NF. The cholangiopathies. *Mayo Clin Proc.* 2015;90(6):791–800.
2. Lazaridis KN, Strazzabosco M, LaRusso NF. The cholangiopathies: Disorders of biliary epithelia. *Gastroenterology* 2004;127(5):1565–77.
3. Gouw AS, Clouston AD, Theise ND. Ductular reactions in human liver: Diversity at the interface. *Hepatology* 2011; 54(5):1853–63.
4. Alpini G, Lenzi R, Sarkozi L, Tavoloni N. Biliary physiology in rats with bile ductular cell hyperplasia. Evidence for a secretory function of proliferated bile ductules. *J Clin Invest.* 1988;81(2):569–78.
5. Slott PA, Liu MH, Tavoloni N. Origin, pattern, and mechanism of bile duct proliferation following biliary obstruction in the rat. *Gastroenterology* 1990;99(2):466–77.
6. Glaser S, Onori P, Wise C, Yang F, Marzioni M, Alvaro D, Franchitto A, Mancinelli R, Alpini G, Munshi MK, and others. Recent advances in the regulation of cholangiocyte proliferation and function during extrahepatic cholestasis. *Dig Liver Dis.* 2010;42(4):245–52.
7. Fickert P, Pollheimer MJ, Beuers U, Lackner C, Hirschfield G, Housset C, Keitel V, Schramm C, Marschall HU, Karlsen TH, and others. International PSC Study Group (IPSCSG). Characterization of animal models for primary sclerosing cholangitis (PSC). *J Hepatol.* 2014;60(6): 1290–303.
8. Hall C, Sato K, Wu N, Zhou T, Kyritsi K, Meng F, Glaser S, Alpini G. Regulators of cholangiocyte proliferation. *Gene Expr.* 2017;17(2):155–71.
9. Maroni L, Haibo B, Ray D, Zhou T, Wan Y, Meng F, Marzioni M, Alpini G. Functional and structural features of cholangiocytes in health and disease. *Cell Mol Gastroenterol Hepatol.* 2015;1(4):368–80.
10. The FO, Boeckxstaens GE, Snoek SA, Cash JL, Bennink R, Larosa GJ, van den Wijngaard RM, Greaves DR, de Jonge WJ. Activation of the cholinergic anti-inflammatory pathway ameliorates postoperative ileus in mice. *Gastroenterology* 2007;133(4):1219–28.

11. Hiramoto T, Chida Y, Sonoda J, Yoshihara K, Sudo N, Kubo C. The hepatic vagus nerve attenuates Fas-induced apoptosis in the mouse liver via alpha7 nicotinic acetylcholine receptor. *Gastroenterology* 2008;134(7):2122–31.
12. Garcia-Ayllon MS, Silveyra MX, Candela A, Compan A, Claria J, Jover R, Perez-Mateo M, Felipe V, Martinez S, Galceran J, and others. Changes in liver and plasma acetylcholinesterase in rats with cirrhosis induced by bile duct ligation. *Hepatology* 2006;43(3):444–53.
13. LeSage G, Alvaro D, Benedetti A, Glaser S, Marucci L, Baiocchi L, Eisel W, Caligiuri A, Phinizz J, Rodgers R, and others. Cholinergic system modulates growth, apoptosis, and secretion of cholangiocytes from bile duct-ligated rats. *Gastroenterology* 1999;117(1):191–9.
14. Morgan ML, Sigala B, Soeda J, Cordero P, Nguyen V, McKee C, Mouralidarane A, Vinciguerra M, Oben JA. Acetylcholine induces fibrogenic effects via M2/M3 acetylcholine receptors in non-alcoholic steatohepatitis and in primary human hepatic stellate cells. *J Gastroenterol Hepatol*. 2016;31(2):475–83.
15. Andersen IM, Tengesdal G, Lie BA, Boberg KM, Karlsen TH, Hov JR. Effects of coffee consumption, smoking, and hormones on risk for primary sclerosing cholangitis. *Clin Gastroenterol Hepatol*. 2014;12(6):1019–28.
16. van Erpecum KJ, Smits SJ, van de Meeberg PC, Linn FH, Wolfhagen FH, vanBerge-Henegouwen GP, Algra A. Risk of primary sclerosing cholangitis is associated with non-smoking behavior. *Gastroenterology* 1996;110(5):1503–6.
17. Hrad V, Abebe Y, Ali SH, Velgersdyk J, Al Hallak M, Imam M. Risk and surveillance of cancers in primary biliary tract disease. *Gastroenterol Res Pract*. 2016;2016:3432640.
18. Tischendorf JJ, Meier PN, Strassburg CP, Klempnauer J, Hecker H, Manns MP, Kruger M. Characterization and clinical course of hepatobiliary carcinoma in patients with primary sclerosing cholangitis. *Scand J Gastroenterol*. 2006;41(10):1227–34.
19. Stinton LM, Shaffer EA. Epidemiology of gallbladder disease: Cholelithiasis and cancer. *Gut Liver* 2012;6(2):172–87.
20. Jensen K, Afroze S, Ueno Y, Rahal K, Frenzel A, Sterling M, Guerrier M, Nizamutdinov D, Dostal DE, Meng F, and others. Chronic nicotine exposure stimulates biliary growth and fibrosis in normal rats. *Dig Liver Dis*. 2013;45(9):754–61.
21. Martinez AK, Jensen K, Hall C, O'Brien A, Ehrlich L, White T, Meng F, Zhou T, Greene J, Jr., Bernuzzi F, and others. Nicotine promotes cholangiocarcinoma growth in xenograft mice. *Am J Pathol*. 2017;187(5):1093–105.
22. Glaser S, Meng F, Han Y, Onori P, Chow BK, Francis H, Venter J, McDaniel K, Marzioni M, Invernizzi P, and others. Secretin stimulates biliary cell proliferation by regulating expression of microRNA 125b and microRNA let7a in mice. *Gastroenterology* 2014;146(7):1795–808.e12.
23. Han Y, Meng F, Venter J, Wu N, Wan Y, Standeford H, Francis H, Meininger C, Greene J, Jr., Trzeciakowski JP, Ehrlich L, Glaser S, Alpini G. miR-34a-dependent overexpression of Per1 decreases cholangiocarcinoma growth. *J Hepatol*. 2016;64(6):1295–304.
24. Smith MJ, Koch GL. Differential expression of murine macrophage surface glycoprotein antigens in intracellular membranes. *J Cell Sci*. 1987;87(Pt 1):113–9.
25. Puche JE, Lee YA, Jiao J, Aloman C, Fiel MI, Munoz U, Kraus T, Lee T, Yee HF, Jr., Friedman SL. A novel murine model to deplete hepatic stellate cells uncovers their role in amplifying liver damage in mice. *Hepatology* 2013;57(1):339–50.
26. Francis H, DeMorrow S, Venter J, Onori P, White M, Gaudio E, Francis T, Greene JF Jr, Tran S, Meininger CJ, Alpini G. Inhibition of histidine decarboxylase ablates the autocrine tumorigenic effects of histamine in human cholangiocarcinoma. *Gut* 2012;61(5):753–64.
27. Feng H, Gerilechaogetu F, Golden HB, Nizamutdinov D, Foster DM, Glaser SS, Dostal DE. p38alpha MAPK inhibits stretch-induced JNK activation in cardiac myocytes through MKP-1. *Int J Cardiol*. 2016;203:145–55.
28. Wu N, Meng F, Invernizzi P, Bernuzzi F, Venter J, Standeford H, Onori P, Marzioni M, Alvaro D, Franchitto A, and others. The secretin/secretin receptor axis modulates liver fibrosis through changes in transforming growth factor-beta1 biliary secretion in mice. *Hepatology* 2016;64(3):865–79.
29. Chiang JYL, Ferrell JM. Bile acid metabolism in liver pathobiology. *Gene Expr*. 2018;18(2):71–87.
30. Altamirano J, Bataller R. Cigarette smoking and chronic liver diseases. *Gut* 2010;59(9):1159–62.
31. Jensen K, Nizamutdinov D, Guerrier M, Afroze S, Dostal D, Glaser S. General mechanisms of nicotine-induced fibrogenesis. *FASEB J*. 2012;26(12):4778–87.
32. Soeda J, Morgan M, McKee C, Mouralidarane A, Lin C, Roskams T, Oben JA. Nicotine induces fibrogenic changes in human liver via nicotinic acetylcholine receptors expressed on hepatic stellate cells. *Biochem Biophys Res Commun*. 2012;417(1):17–22.
33. Albuquerque EX, Pereira EFR, Alkondon M, Rogers SW. Mammalian nicotinic acetylcholine receptors: From structure to function. *Physiol Rev*. 2009;89(1):73–120.
34. Rhoades RA, Bell DR. Autonomic nervous system medical physiology: Principles for clinical medicine, 4th edition. Baltimore (MD): Wolters Kluwer Business; 2013.
35. Kimura K, Tanida M, Nagata N, Inaba Y, Watanabe H, Nagashimada M, Ota T, Asahara S, Kido Y, Matsumoto M, and others. Central insulin action activates Kupffer cells by suppressing hepatic vagal activation via the nicotinic alpha 7 acetylcholine receptor. *Cell Rep*. 2016;14(10):2362–74.
36. Nishio T, Taura K, Iwaisako K, Koyama Y, Tanabe K, Yamamoto G, Okuda Y, Ikeno Y, Yoshino K, Kasai Y, and others. Hepatic vagus nerve regulates Kupffer cell activation via alpha7 nicotinic acetylcholine receptor in nonalcoholic steatohepatitis. *J Gastroenterol*. 2017;52(8):965–76.
37. Heinrich S, Georgiev P, Weber A, Vergopoulos A, Graf R, Clavien PA. Partial bile duct ligation in mice: A novel model of acute cholestasis. *Surgery* 2011;149(3):445–51.
38. Marzioni M, LeSage G, Glaser S, Patel T, Marienfeld C, Ueno Y, Francis H, Alvaro D, Tadlock L, Benedetti A, and others. Taurocholate prevents the loss of intrahepatic bile ducts due to vagotomy in bile duct-ligated rats. *Am J Physiol Gastrointest Liver Physiol*. 2003;284(5):G837–52.
39. Kaminski DL, Dorigi J, Jellinek M. Effect of electrical vagal stimulation on canine hepatic bile flow. *Am J Physiol*. 1974;227(2):487–93.
40. Elsing C, Hubner C, Fitscher BA, Kassner A, Stremmel W. Muscarinic acetylcholine receptor stimulation of biliary epithelial cells and its effect on bile secretion in the isolated perfused liver [corrected]. *Hepatology* 1997;25(4):804–13.
41. Alvaro D, Alpini G, Jezequel AM, Bassotti C, Francia C, Fraioli F, Romeo R, Marucci L, Le Sage G, Glaser S, and others. Role and mechanisms of action of acetylcholine in

- the regulation of rat cholangiocyte secretory functions. *J Clin Invest.* 1997;100(6):1349–62.
42. Wang B, Dolinski BM, Kikuchi N, Leone DR, Peters MG, Weinreb PH, Violette SM, Bissell DM. Role of $\alpha v \beta 6$ integrin in acute biliary fibrosis. *Hepatology* 2007;46(5):1404–12.
43. Patsenker E, Popov Y, Stickel F, Jonczyk A, Goodman SL, Schuppan D. Inhibition of integrin $\alpha v \beta 6$ on cholangiocytes blocks tgfbeta activation and retards biliary fibrosis progression. *Gastroenterology* 2008;135(2):660–70.
44. Georges PC, Hui JJ, Gombos Z, McCormick ME, Wang AY, Uemura M, Mick R, Janmey PA, Furth EE, Wells RG. Increased stiffness of the rat liver precedes matrix deposition: Implications for fibrosis. *Am J Physiol Gastrointest Liver Physiol.* 2007;293(6):G1147–54.